

# Approximate Message Passing with Restricted Boltzmann Machine Priors

Eric W. Tramel, Angélique Drémeau, and Florent Krzakala

## Abstract

Approximate Message Passing (AMP) has been shown to be an excellent statistical approach to signal inference and compressed sensing problem. The AMP framework provides modularity in the choice of signal prior; here we propose a hierarchical form of the Gauss-Bernouilli prior which utilizes a Restricted Boltzmann Machine (RBM) trained on the signal support to push reconstruction performance beyond that of simple i.i.d. priors for signals whose support can be well represented by a trained binary RBM. We present and analyze two methods of RBM factorization and demonstrate how these affect signal reconstruction performance within our proposed algorithm. Finally, using the MNIST handwritten digit dataset, we show experimentally that using an RBM allows AMP to approach oracle-support performance.

## I. INTRODUCTION

Over the past decade, a groundswell in research has occurred in both difficult inverse problems, such as those encountered in Compressed Sensing (CS) [1], and in signal representation and classification via deep networks. In recent years, Approximate Message Passing (AMP) [2] has been shown to be a near-optimal, efficient, and extensible application of belief propagation to solving inverse problems which admit a statistical description.

While AMP has enjoyed much success in solving problems for which an i.i.d. signal prior is known, only a few works have investigated the application of AMP to more complex, structured priors. Utilizing such complex priors is key to leveraging many of the advancements recently

E. W. Tramel is with Laboratoire de Physique Statistique, UMR 8550 CNRS & École Normale Supérieure 24 rue Lhomond, 75005 Paris, France.

A. Drémeau is with ENSTA Bretagne 2 rue François Verny, 29806 Brest, France.

F. Krzakala is with Laboratoire de Physique Statistique, UMR 8550 CNRS & École Normale Supérieure Université Pierre et Marie Curie, Sorbonne Universités 24 rue Lhomond, 75005 Paris, France.

seen in statistical signal representation. Techniques such as GRAMPA [3] and Hybrid AMP [4] have shown promising results when incorporating correlation models directly between the signal coefficients, and in fact the present contribution is similar in spirit to Hybrid AMP.

Another possible approach is to not attempt to model the correlations directly, but instead to utilize a bipartite construction via hidden variables, as in the Restricted Boltzmann Machine (RBM) [5]. As we will show, if a binary RBM can be trained to model the support pattern of a given signal class, then the statistical description of the RBM easily admits its use within AMP. This is particularly interesting since RBMs are the building blocks of “deep belief networks” [6] and have recently sparked a surge of interest, partly because of the efficient algorithms developed to train them (e.g. Contrastive Divergence (CD) [7]). The present paper demonstrates the first steps in incorporating deep learned priors into generalized linear problems such as compressed sensing.

The paper is organized as follows. We first review factorizations of RBM-based priors based upon free energy approximations as well as the AMP framework in Section II. Next, we propose a method by which to couple AMP iteration with an RBM prior on a signal’s support in Section III-A, giving a detailed description of the subsequent algorithm in Section III-B. We then demonstrate the effectiveness of using the RBM for modeling signal support using the MNIST handwritten digit database in Section IV.

## II. BACKGROUND

### A. *Approximate Message Passing*

Loopy Belief Propagation (BP) is a powerful iterative message passing algorithm for graphical models [8, 9]. However, it presents two main drawbacks when applied to highly-connected, continuous-variable problems such as CS: first, the need to work with continuous probability distributions; and second, the necessity to iterate over one such probability distribution for each pair of variables. These problems can be addressed by projecting the distributions on to their first two moments and by approximating the messages by the marginals. Applying both to BP for the CS problem, one obtains the AMP iteration.

AMP has been shown to be a very powerful algorithm for CS signal recovery, especially in the probabilistic context with prior information. In CS, one has the following forward model to

obtain set of  $M$  observations  $\mathbf{y}$ ,

$$y_\mu = \sum_{i=1}^N F_{\mu i} x_i + w_\mu \quad \text{where} \quad w_\mu \sim \mathcal{N}(0, \Delta)^1, \quad (1)$$

where  $F$  is an  $M \times N$  matrix, for  $M \ll N$ , representing linear observations of an unknown signal  $\mathbf{x}$  which are then corrupted by an additive zero-mean white Gaussian noise (AWGN) of some variance  $\Delta$ .

We can utilize AMP to estimate a factorization, up to the first two moments, of the posterior distribution

$$P(\mathbf{x}|F, \mathbf{y}) \propto P_0(\mathbf{x})P(\mathbf{y}|F, \mathbf{x}), \quad (2)$$

where  $P(\mathbf{y}|F, \mathbf{x})$  is defined by the likelihood of an observation from the AWGN channel and  $P_0(\mathbf{x})$  is a prior on the signal, so that we can obtain the MMSE estimate of  $\mathbf{x}$ ,

$$\hat{x}_i^{\text{MMSE}} = \int dx_i \ x_i P(x_i|F, \mathbf{y}), \quad \forall i. \quad (3)$$

We are mainly interested in the case where the signal  $\mathbf{x}$  is *sparse*, that is, very few of its coefficients are non-zero. One can perform sparse signal recovery from CS measurements by using a sparse Gauss-Bernoulli (GB) prior,

$$P_0(\mathbf{x}) = \prod_i (1 - \rho) \delta(x_i) + \frac{\rho}{\sqrt{2\pi\sigma^2}} e^{-\frac{(x_i - \mu)^2}{2\sigma^2}}. \quad (4)$$

When using this prior, the accuracy of the final MMSE estimate is dependent upon the relationship between the sparsity of the unknown signal  $\rho$  and the measurement rate,  $\alpha = M/N$ .

We refer the reader to [2, 10–13] and in particular to [14] for the present notation and the derivation of AMP from BP and we give directly the iterative form of the algorithm. Given the current estimate of the factorized posterior mean  $a_i$  and variance  $c_i$  for each variable, a single

<sup>1</sup>In the present work, we use subscript notation to denote the individual coefficients of vectors, i.e.  $y_\mu$  refers to the  $\mu^{\text{th}}$  coefficient of  $\mathbf{y}$  and the double-subscript notation to refer to individual matrix elements in row-column order.

step of AMP iteration reads

$$V_\mu^{t+1} = \sum_i F_{\mu i}^2 c_i^t, \quad (5)$$

$$\omega_\mu^{t+1} = \sum_i F_{\mu i} a_i^t - (y_\mu - \omega_\mu^t) \frac{V_\mu^{t+1}}{\Delta + V_\mu^t}, \quad (6)$$

$$(\Sigma_i^{t+1})^2 = \left[ \sum_\mu \frac{F_{\mu i}^2}{\Delta + V_\mu^{t+1}} \right]^{-1}, \quad (7)$$

$$R_i^{t+1} = a_i^t + (\Sigma_i^{t+1})^2 \sum_\mu F_{\mu i} \frac{(y_\mu - \omega_\mu^{t+1})}{\Delta + V_\mu^{t+1}}. \quad (8)$$

Once the new values of  $R_i$  and  $\Sigma_i^2$  are computed, the new estimates of the posterior mean and variance,  $a_i$  and  $c_i$ , given the prior  $P_0(\mathbf{x})$ , are calculated as

$$a_i^{t+1} \triangleq \int dx_i \frac{x_i}{\mathcal{Z}_i} P_0(x_i) e^{-\frac{(x_i - R_i)^2}{2\Sigma_i^2}}, \quad (9)$$

$$c_i^{t+1} \triangleq \int dx_i \frac{x_i^2}{\mathcal{Z}_i} P_0(x_i) e^{-\frac{(x_i - R_i)^2}{2\Sigma_i^2}} - (a_i^{t+1})^2, \quad (10)$$

where  $\mathcal{Z}_i$  is a normalization constant. While we note the i.i.d. GB prior in Eq. (4), since Eqs. (9) and (10) are not specific to any particular prior, one could in principle use a more complicated prior, even one involving a joint probability distribution, by trivially generalizing Eqs. (9) and (10). Indeed, there has been some activity in developing iterative algorithms with structured, non-factorized, priors [4, 15, 16]. We continue along this path by incorporating an RBM prior into AMP in Section III.

### B. Approximated Free Energies for the Binary RBM

A restricted Boltzmann machine is an Energy based model similar to what is called an Ising model on a bipartite graph in statistical physics. The joint probability distribution over the visible and hidden layers for the RBM is given by an energy based-model

$$P(\mathbf{v}, \mathbf{h}) \propto e^{-E(\mathbf{v}, \mathbf{h})}, \quad (11)$$

where the energy  $E(\mathbf{v}, \mathbf{h})$  reads

$$E(\mathbf{v}, \mathbf{h}) = - \sum_i b_i^v v_i - \sum_j b_j^h h_j - \sum_{i,j} \mathbf{W}_{i,j} v_i h_j. \quad (12)$$

The RBM model is described by the two sets of biasing coefficients  $\mathbf{b}^v$  and  $\mathbf{b}^h$  on the visible and hidden layers, respectively, and the learned connections between the layers represented by the matrix  $\mathbf{W}$ .

In the sequel, we leverage the connection between the RBM and the well known results of statistical physics to discuss a simplification of the RBM under the so-called mean-field approximation (MFA), as well as a better approximation known as Thouless-Anderson-Palmer (TAP) [17–19], in order to obtain factorizations over the visible and hidden layers from this joint distribution.

1) *The mean-field approach:* Given the value of an Energy-function  $E(\{\mathbf{x}\})$ , also called Hamiltonian in physics, a standard technique is to use the Gibbs variational approach where the Gibbs free energy  $\mathcal{F}$  is minimized over a trial distribution,  $P_{\text{var}}$ , with

$$\mathcal{F}(\{P_{\text{var}}\}) = \langle E(\{\mathbf{x}\}) \rangle_{\{P_{\text{var}}\}} - S_{\text{Gibbs}}(P_{\text{var}}) \quad (13)$$

where  $\langle \cdot \rangle_{\{P_{\text{var}}\}}$  denotes the average over distribution  $P_{\text{var}}$  and  $S_{\text{Gibbs}}$  is the Gibbs entropy.

It is instructive to first review the simplest variational solution, namely, the mean field one, where  $P_{\text{var}} = \prod_i Q_i(x_i)$ . Within this ansatz, a classical computation shows that the free energy, in the case of the binary RBM, reads as

$$\begin{aligned} \mathcal{F}_{\text{MFA}}^{\text{RBM}}(\bar{\mathbf{v}}, \bar{\mathbf{h}}) &= - \sum_i b_i^v \bar{v}_i - \sum_j b_j^h \bar{h}_j - \sum_{\langle i,j \rangle} \mathbf{W}_{i,j} \bar{v}_i \bar{h}_j \\ &+ \sum_i [\text{H}(\bar{v}_i) + \text{H}(1 - \bar{v}_i)] + \sum_j [\text{H}(\bar{h}_j) + \text{H}(1 - \bar{h}_j)], \end{aligned} \quad (14)$$

where  $H(x) = x \ln(x)$  and

$$\bar{v}_i = \mathbb{E}[v_i] = \text{Prob}[v_i = 1], \quad (15)$$

which also tells us that  $\text{Prob}[v_i = 0] = 1 - \bar{v}_i$ . Since the hidden variables are also binary in

nature, these identities are equally true for  $\bar{h}_j$ .

Of particular interest in this case are the fixed points of the means of both the visible and the hidden variables. With these fixed points we can calculate a factorization for both  $P(\mathbf{v})$  and  $P(\mathbf{h})$ , depending on the desired application. First, we look at the partials of the MFA free energy for the RBM w.r.t. the visible and hidden sites, which, evaluated at the critical point, give us the following fixed-point conditions for the expected values of the variables:

$$\bar{v}_i = \text{sigm}(b_i^v + \sum_j \mathbf{W}_{i,j} \bar{h}_j), \quad (16)$$

$$\bar{h}_j = \text{sigm}(b_j^h + \sum_i \mathbf{W}_{i,j} \bar{v}_i), \quad (17)$$

where  $\text{sigm}(x)$  is the sigmoid function defined as

$$\text{sigm}(x) = [1 + e^{-x}]^{-1}. \quad (18)$$

These equations are in line with the assumed MFA fixed-point conditions used for finding the “site activations” given in the RBM literature. In fact, they are often use as iterative equation to find the minimum free energy.

2) *Thouless-Anderson-Palmer approach*: A classical tool in spin glass theory and in statistical physics is the Thouless-Anderson-Parlmer (TAP) one [17, 18], which improves on the mean-field approach by taking into account further correlations. In fact, in many situations, the improvement is drastic, making the TAP approach a very popular one in statistical inference [19].

There are many way in which the TAP equations can be presented, and we shall refer, for the sake of the presentation, to the known results of the statistical physics community. One possible way to derive the TAP approach is to recognize that the mean-field free energy is merely the first term in a perturbative expansion in power of the coupling constants  $\mathbf{W}$ , as was shown by Plefka [20], and to keep the second order term. Alternatively, one may start with the Bethe approximation and use the fact that the system is densely connected [18, 19]. Proceeding according to Plefka, the TAP free energy reads

$$\mathcal{F}_{\text{TAP}}^{\text{RBM}}(\bar{\mathbf{v}}, \bar{\mathbf{h}}) = \mathcal{F}_{\text{MFA}}^{\text{RBM}}(\bar{\mathbf{v}}, \bar{\mathbf{h}}) - \frac{1}{2} \sum_{\langle i,j \rangle} \mathbf{W}_{i,j}^2 \hat{v}_i \hat{h}_j. \quad (19)$$

where we have denoted the variances of hidden and visible variables,  $\hat{\mathbf{h}}$  and  $\hat{\mathbf{v}}$ , respectively, as

$$\hat{h}_j = \mathbb{E} [h_j^2] - \mathbb{E} [h_j]^2 = \bar{h}_j - \bar{h}_j^2, \quad (20)$$

$$\hat{v}_i = \mathbb{E} [v_i^2] - \mathbb{E} [v_i]^2 = \bar{v}_i - \bar{v}_i^2. \quad (21)$$

Repeating the extremisation, one finds

$$\bar{v}_i = \text{sigm} \left( b_i^v + \sum_j \mathbf{W}_{i,j} \bar{h}_j + \left( \frac{1}{2} - \bar{v}_i \right) \sum_j \mathbf{W}_{i,j}^2 \hat{h}_j \right), \quad (22)$$

$$\bar{h}_j = \text{sigm} \left( b_j^h + \sum_i \mathbf{W}_{i,j} \bar{v}_i + \left( \frac{1}{2} - \bar{h}_j \right) \sum_i \mathbf{W}_{i,j}^2 \hat{v}_i \right). \quad (23)$$

Eqs. (22) and (23), often called the TAP equations, can be seen as an extension of the mean field iteration of Eqs. (16) and (17). The additional term is called the Onsager retro-action term in statistical physics [18]. In fact, these are the tools one uses in order to derive AMP itself. Given an RBM model, we now have two approximated solutions to obtain the equilibrium marginal through the iteration of either Eqs. (16) and (17) or Eqs. (22) and (23). As we shall see later, the TAP approach does indeed improve on the mean-field one.

### III. RBMS FOR AMP

#### A. RBM-based Support Estimation

The scope of this work is to use the RBM model within the AMP framework. Here, we would like to utilize the binary RBM to give us information on each site's likelihood of being *on-support*, that is, its probability to be a non-zero coefficient. This shoehorns nicely into our sparse GB prior in Eq. (4).

This prior is defined for the given scalar parameters  $\rho$ ,  $\mu$ , and  $\sigma^2$ . Here,  $\rho$  represents the probability of  $x_i$  to be non-zero, i.e. *on-support*. If, rather than a fixed probability of being on-support for all sites, we instead have a probability for each specific site to be on-support, we could easily modify Eq. (4),

$$P(\mathbf{x}; \{\rho_i\}) = \prod_i (1 - \rho_i) \delta(x_i) + \frac{\rho_i}{\sqrt{2\pi\sigma^2}} e^{-\frac{(x_i - \mu)^2}{2\sigma^2}}. \quad (24)$$

This change in the prior must also be reflected in the partition function utilized in Eqs. (9) and

(10),

$$\begin{aligned}
\mathcal{Z}_i &= \int dx_i P(x_i; \rho_i) \mathcal{N}(x_i; R_i, \Sigma_i^2), \\
&= (1 - \rho_i) \exp \left\{ -\frac{R_i^2}{2\Sigma_i^2} \right\} \\
&\quad + \rho_i \sqrt{\frac{\Sigma_i^2}{\Sigma_i^2 + \sigma^2}} \exp \left\{ -\frac{(R_i - \mu)^2}{2(\Sigma_i^2 + \sigma^2)} \right\}, \\
&= (1 - \rho_i) \mathcal{Z}_i^z + \rho_i \mathcal{Z}_i^{\text{nz}},
\end{aligned} \tag{25}$$

where, for later convenience, we write the partition using these two sub-partition terms related to the zero (off-support) and non-zero (on-support) probabilities. From this partition function, for a given setting of  $R_i$  and  $\Sigma_i^2$  (which result from the AMP evolution), we can write the posterior means and variances,  $\mathbf{a}$  and  $\mathbf{c}$ .

A nice feature of this two-part prior is that it also admits a natural estimation of the probability of a particular coefficient to be on- or off-support. Specifically, at a given point in the AMP evolution, if the support set of the signal is denoted as  $\mathcal{S}$ ,

$$\begin{aligned}
\text{Prob}^{\text{AMP}} [x_i \in \mathcal{S}] &= \rho_i \frac{\mathcal{Z}_i^{\text{nz}}}{\mathcal{Z}_i}, \\
\text{Prob}^{\text{AMP}} [x_i \notin \mathcal{S}] &= (1 - \rho_i) \frac{\mathcal{Z}_i^z}{\mathcal{Z}_i}.
\end{aligned} \tag{26}$$

In fact, we see that, if we have a prior model for the probability of the variable to be off- and on-support, given by  $P(v_i)$  with  $v_i \in \{0, 1\}$  and  $P(1) = \rho_i$ , we can see that the additional information given by AMP about the support probability results in a modified support probability of

$$\tilde{P}(v_i) \propto P(v_i) e^{\gamma_i v_i} \tag{27}$$

where  $\gamma_i$  is the ratio of the on- to off-support partitions,  $\gamma_i = \frac{\mathcal{Z}_i^{\text{nz}}}{\mathcal{Z}_i^z}$ , which gives us the following equation for its natural logarithm

$$\ln \gamma_i = \frac{R_i^2}{2\Sigma_i^2} - \frac{(R_i - \mu)^2}{2(\Sigma_i^2 + \sigma^2)} + \ln \sqrt{\frac{\Sigma_i^2}{\Sigma_i^2 + \sigma^2}}. \tag{28}$$

The next question is, of course: how does one choose  $P(v_i)$ ? We propose the use of an RBM.



Since in this case  $P(v_i)$  has the classical exponential form of an Energy-based model, we see that the addition of the information provided by AMP simply amounts to an additional local bias (or field) on the visible variables equal to  $\ln \gamma_i$ . That is, the AMP-modified RBM free energy is simply the introduction of an additional field term along with a constant bias,

$$\mathcal{F}^{\text{RBM-AMP}}(\bar{\mathbf{v}}, \bar{\mathbf{h}}) = \mathcal{F}^{\text{RBM}}(\bar{\mathbf{v}}, \bar{\mathbf{h}}) - \sum_i \bar{v}_i \ln \gamma_i. \quad (29)$$

As we can see, this field effect only exists on the visible layer of the RBM. Because of this, the AMP framework does not put any extra influence on the hidden layer, but only on the visible layer. Thus, the fixed point of the hidden layer means is not influenced by AMP, but the visible ones are. With respect to (16) and (22), the AMP-modified fixed points of the the visible variable means contain one additional additive term within the sigmoid, giving

$$\bar{v}_i = \text{sigm}(b_i^v + \ln \gamma_i + \sum_j \mathbf{W}_{i,j} \bar{h}_j), \quad (30)$$

for the MFA-based fixed point, and

$$\begin{aligned} \bar{v}_i = \text{sigm}(b_i^v + \ln \gamma_i + \sum_j \mathbf{W}_{i,j} \bar{h}_j \\ + \left(\frac{1}{2} - \bar{v}_i\right) \sum_j \mathbf{W}_{i,j}^2 \hat{h}_j), \end{aligned} \quad (31)$$

for the TAP one.

### B. Integration into AMP

The most direct approach for factorizing the AMP influenced RBM is to construct a fixed-point iteration (FPI) using the MFA or TAP fixed-point conditions detailed in Section III-A. Given some initial condition for  $\bar{\mathbf{v}}$  and  $\bar{\mathbf{h}}$ , we can successively estimate the visible and hidden layers via their respective fixed-point equations.

Because of the sigmoid functions in the fixed-point conditions, such a FPI will not diverge. However, it is possible that the FPI will arrive at one of the two trivial solutions for the factorization, that is, all 1's or all 0's. Whether or not the FPI arrives at these trivial points relies on the balance between the evolution of the FPI and the contributing fields, in this case, the RBM biases and the AMP influence.

---

**Algorithm 1** AMP with RBM Support Prior
 

---

**Input:**  $F, \mathbf{y}, \mathbf{W}, \mathbf{b}^v, \mathbf{b}^h$   
*Initialize:*  $\mathbf{a}, \mathbf{c}, \{\rho_i\}$   
**repeat**  
   AMP Update on  $\{V_\mu, \omega_\mu\}$  via (5) and (6)  $\forall \mu$   
   AMP Update on  $\{R_i, \Sigma_i^2\}$  via (8) and (7)  $\forall i$   
   Calculate  $\ln \gamma_i$  via (28)  $\forall i$   
   *Initialize:*  $\bar{h}_j, \hat{h}_j = 0 \quad \forall j$   
   *Initialize:*  $\bar{v}_i = \rho_i \quad \forall i$   
   **repeat**  
     Update  $\bar{h}_j$  via (17) or (23)  $\forall j$   
     Update  $\bar{v}_i$  via (30) or (31)  $\forall i$   
   **until** Convergence on  $\bar{\mathbf{v}}$   
    $\rho_i \leftarrow \bar{v}_i \quad \forall i$   
   AMP Update on  $a_i$  using  $\rho_i$  via (9)  $\forall i$   
   AMP Update on  $c_i$  using  $\rho_i$  via (10)  $\forall i$   
**until** Convergence on  $\mathbf{a}$

---

Additionally, it is not entirely clear in which order one should iterate these two fixed-point equations. However, it seems most intuitive to construct the iteration using an update on  $\bar{\mathbf{h}}$  followed by the update on  $\bar{\mathbf{v}}$ . This follows since we know the value of the influencing field on  $\bar{\mathbf{v}}$  coming from AMP, but we do not have any assumptions or prior expectation on what the values of the hidden layer should be. And so, if one starts the iteration with  $\bar{\mathbf{v}}$ , this requires either using  $\bar{\mathbf{h}}$  with 0 as an initial value, or making up a random set of activations. The random activations could influence our result unduly, and starting from a 0 activation for all hidden variables results in the hidden-to-visible iteration we suggest.

We give the final construction of the AMP algorithm with the RBM support prior in Alg. 1. Some initial values are required to start the iteration, namely, for  $\mathbf{a}$ ,  $\mathbf{c}$ , and the set of per-coefficient sparsity terms  $\{\rho_i\}$ . The proposed algorithm is not sensitive to these initial conditions beyond that of the standard AMP iteration.

#### IV. NUMERICAL RESULTS WITH MNIST

To show the efficacy of the proposed RBM-based support prior within the AMP framework, we conduct a series of experiments using the MNIST database of handwritten digits. Each sample of the database is a  $20 \times 20$  pixel image of a digit with values in the range  $[0, 1]$ . For the following experiments, an RBM with 1000 hidden variables was trained on 10,000 training samples from

the MNIST training set. In order to build an RBM model of the support of these handwritten digits, the training data was thresholded so that all non-zero pixels were given a value of 1.

Following the prescription of [21] for generative RBM models on the binary MNIST dataset, a learning rate of 0.005 was used in conjunction with 50 training epochs. The training of the RBM was achieved via contrastive divergence [5]. To test CS reconstruction performance, we drew 1000 testing samples from the 10000 training samples. While not strictly enforced, the sampling of each class of digit is approximately uniform.

Given the large number of hidden units, and the way in which we draw the samples for reconstruction, we acknowledge that this represents an unrealistic application of an RBM. In general, one would expect that the reconstruction test set would not be known *a priori* for the RBM training. However, our goal in these experiments is to simply show that an RBM can indeed be used within the AMP framework, and we would like to show the possible reconstruction performance when the trained RBM model matches the tested support well. Because the reconstruction performance is very dependent upon the ability of the RBM to represent the signal support, we did not want to misjudge the potential of the proposed approach by using an inadequate RBM model. We leave open the question of what exactly makes an adequately trained RBM signal-support model in terms of the number of measurements needed for successful signal recovery and point out that this is an interesting topic for future analytical works.

Once the RBM model for the support is known, we construct a series of CS reconstruction tests. In these tests, ensembles of Gaussian i.i.d. linear projections were used to generate the CS measurements. To gain an understanding of the comparison of the algorithms in an optimal setting, we set the AWGN variance to a small value of  $\Delta = 10^{-8}$ . Additionally, we assume that this noise variance is known to all of the tested approaches, however, the per-iteration estimation of the noise variance is allowed to change in each of the three tested approaches according to the fixed-point estimate of  $\Delta$  given in [14].

When using the RBM priors on the signal support, the convergence criterion on  $\bar{\mathbf{v}}$  was calculated as a MSE difference of  $10^{-7}$ . Additionally, no damping was used within the RBM factorization itself, however, a significant damping was applied to the AMP update on  $R_i$  and  $\Sigma_i^2$ .

For comparison, along with testing AMP using the MFA and TAP RBM factorizations, (RBM

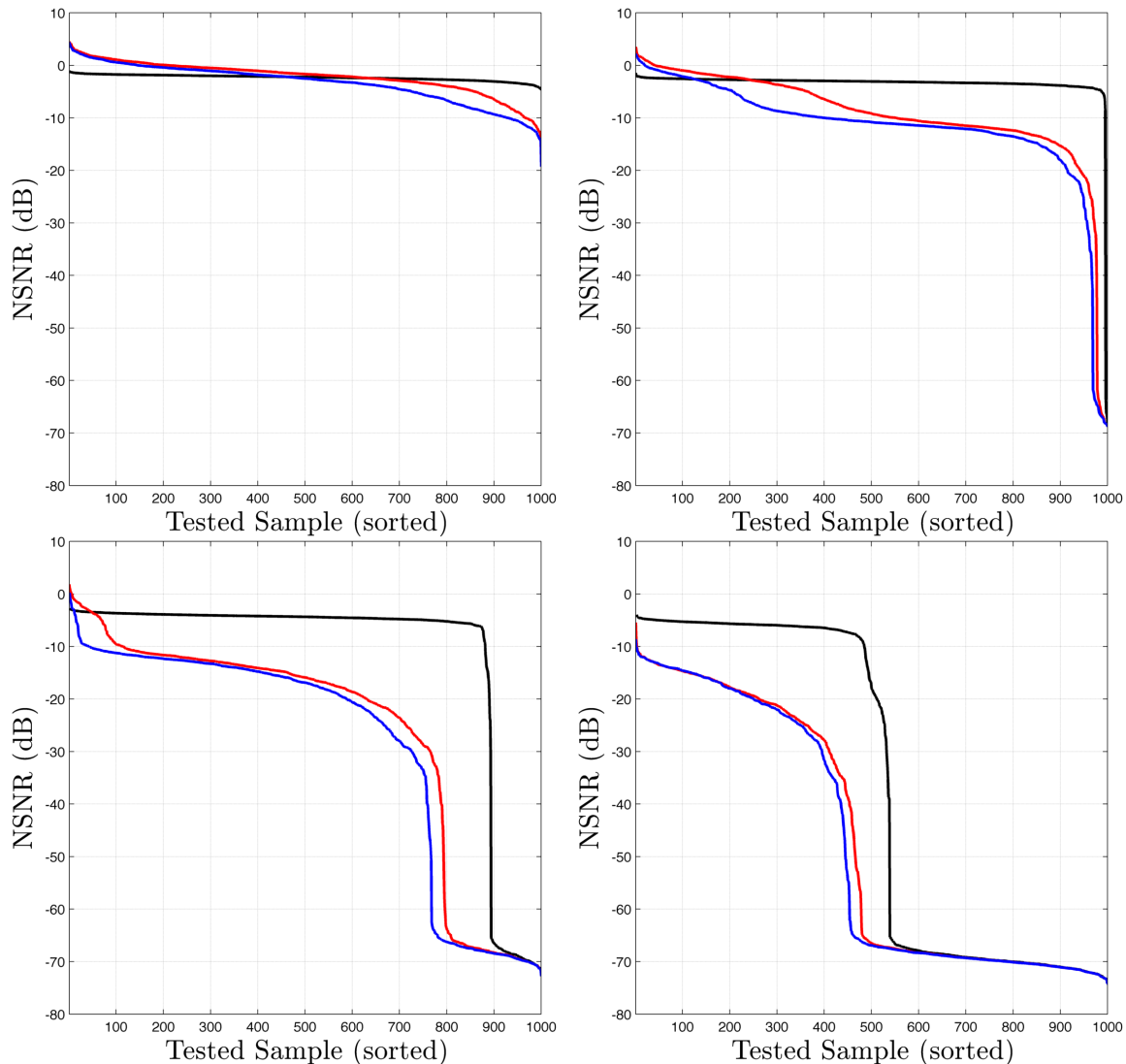


Fig. 1. Comparison over tested MNIST handwritten digits for reconstruction performance in terms of NSNR for  $\alpha = 0.15$  (top left),  $\alpha = 0.25$  (top right),  $\alpha = 0.35$  (bottom left), and  $\alpha = 0.45$  (bottom right). Black curve: AMP using GB prior. Red curve: AMP using RBM (MF) support prior. Blue curve: AMP using RBM (TAP) support prior.

(MF) and RBM (TAP), respectively), we also investigate the reconstruction of the same data using the GB prior with no extra information about the support location. In this case, the true value of  $\rho$ , evaluated as the total support in each image over the number of pixels, was assumed to be known.

Before looking at the performance comparisons, we first note the per-digit-class average sparsity in Table I. These sparsity levels inform us of the limit on the number of measurements required to accurately recovery each class of handwritten digits, on average. The optimal perfor-

TABLE I  
 CLASSES OF HANDWRITTEN DIGITS IN THE TESTED SUBSET OF THE MNIST DATABASE SORTED ACCORDING TO THE AVERAGE SPARSITY OF EACH DIGIT CLASS. THE AVERAGE SPARSITY IS REPORTED ALONG WITH THE STANDARD DEVIATION OF THE SPARSITY ACROSS ALL SAMPLES OF THE DIGIT CLASS.

DIGIT CLASS	$\rho$
“1”	$0.200 \pm 0.050$
“7”	$0.277 \pm 0.064$
“9”	$0.309 \pm 0.069$
“4”	$0.313 \pm 0.067$
“5”	$0.321 \pm 0.078$
“6”	$0.340 \pm 0.076$
“3”	$0.362 \pm 0.085$
“2”	$0.373 \pm 0.082$
“8”	$0.377 \pm 0.076$
“0”	$0.441 \pm 0.086$

mance of our approach would be an oracle RBM which always reports the true signal support at each AMP iteration. If the signal support were truly known, only  $M = K$  measurements would be required for successful signal reconstruction, where  $K$  is the number of non-zero coefficients. From this table, in terms of the number of measurements required for accurate reconstruction, we expect that digit class “1” should be the easiest to recover, while digit class “0” will be the most difficult.

In Fig. 1, we see the reconstruction performance, in terms of the normalized signal-to-noise ratio (NSNR), for all of the tested samples using each of the three approaches, sorted according to accuracy. The NSNR is calculated in decibels as

$$\text{NSNR}(\mathbf{x}, \hat{\mathbf{x}}) = 10 \log_{10} \frac{\|\mathbf{x} - \hat{\mathbf{x}}\|_2^2}{\|\mathbf{x}\|_2^2}, \quad (32)$$

with smaller values representing a more accurate reconstruction. Using the NSNR metric, digits reconstructed at  $\leq -15$  dB are easily recognizable, hence, we choose this level of NSNR to represent a “successful reconstruction” of an MNIST sample image in our experiments.

One can see in Fig. 1(a) that AMP using the i.i.d. GB prior exhibits a strong first-order phase transition at each of the tested measurement rates. That is, the reconstructed digit images fall into only two categories, those which are successfully recovered, and those which are not. Whether or not a digit image is successfully recovered at a particular measurement rate is entirely dependent upon the sparsity of the particular digit image. As the measurement rate increases, we see that

TABLE II  
 RECONSTRUCTION SUCCESS RATES FOR THE HANDWRITTEN DIGIT TEST SET OVER MEASUREMENT RATE FOR DIFFERENT CLASSES OF DIGITS. A SUCCESSFUL RECONSTRUCTION IS DENOTED AS A RECONSTRUCTION WHICH ACHIEVES AN NSNR  $\leq -15$  dB.

ALL DIGITS	$\alpha$	0.15	0.25	0.35	0.45
GB		0.0%	0.5%	11.3%	50.6%
RBM (MF)		0.1%	10.6%	53.6%	88.7%
RBM (TAP)		0.1%	14.7%	58.9%	88.1%
“1” DIGITS	$\alpha$	0.15	0.25	0.35	0.45
GB		0.0%	3.5%	61.1%	99.1%
RBM (MF)		0.9%	51.3%	92.9%	100.0%
RBM (TAP)		0.9%	69.9%	98.2%	100.0%
“7” DIGITS	$\alpha$	0.15	0.25	0.35	0.45
GB		0.0%	0.0%	16.4%	79.5%
RBM (MF)		0.0%	23.0%	88.5%	100.0%
RBM (TAP)		0.0%	27.9%	93.4%	100.0%
“5” DIGITS	$\alpha$	0.15	0.25	0.35	0.45
GB		0.0%	0.0%	9.2%	62.1%
RBM (MF)		0.0%	1.1%	52.9%	94.3%
RBM (TAP)		0.0%	5.7%	65.5%	94.3%
“2” DIGITS	$\alpha$	0.15	0.25	0.35	0.45
GB		0.0%	0.0%	2.1%	33.0%
RBM (MF)		0.0%	3.2%	21.3%	83.0%
RBM (TAP)		0.0%	3.2%	34.0%	83.0%
“0” DIGITS	$\alpha$	0.15	0.25	0.35	0.45
GB		0.0%	0.0%	0.0%	7.4%
RBM (MF)		0.0%	0.0%	14.9%	55.3%
RBM (TAP)		0.0%	0.0%	16.0%	53.2%

the transition shifts and more digit images are recovered successfully. This is entirely in keeping with the known behavior of the AMP algorithm using the GB prior.

For Figs. 1(b) and 1(c), we observe that the the reconstruction performances of the RBM (MF) and RBM (TAP) are quite close, with a slight advantage going to RBM (TAP). The major feature of interest, however, is that when using AMP with the RBM support prior no first-order phase transition is apparent. Instead, we see that across the tested samples, there is a gradient of reconstruction performance between useless and exact reconstruction. And, specifically in terms of successful reconstructions ( $\leq -15$  dB), a much larger percentage of the reconstructions are useful when using the RBM (MF) or RBM (TAP) as compared to the GB prior.

Next, in Table II we note the rates of successful reconstruction at each of the tested measurement rates when using the GB, RBM (MF), and RBM (TAP) priors. Along with reporting the

success rates across all of the tested classes of digit images, we also show results for certain classes of digits in increasing order of difficulty (as noted in Table I). We can easily observe the distinct advantage that the RBM support prior gives in terms of the successful reconstruction rate. For example, for the hardest digit class, “0”, using AMP with an RBM prior allows for successful reconstruction of the majority of the tested digits at  $\alpha = 0.45$  whereas the reconstruction of this digit class is not possible at any of the tested rates when using the GB prior.

We compare the results presented in Table II with the known AMP-GB [14] and support-oracle phase transitions in Fig. 2. We first note that neither the GB nor the RBM priors provide successful digit class reconstruction below the oracle support transition. However, when using the RBM prior, successful reconstruction of the shown digit classes is possible much closer to the oracle transition than when using the GB prior. We note that the comparison here between these empirical results on MNIST and the theoretical lines is not an exact comparison due to a number of factors, including finite size effects, the effects of averaging across samples of different sparsities within each digit class, as well as a difference in how “success” is estimated between the replica obtained AMP-GB transition and how we define success for these experiments.

Finally, Fig. 3, we can see a visual comparison of the reconstruction performance of the three approaches for a single instance of a digit image reconstruction at five different measurement rates. Looking at the digit images recovered using the GB prior, we see that all of the reconstructions fail until the number of measurements exceeds the phase transition for AMP-GB. Once past this point, for  $\alpha = 0.55$ , we see an exact reconstruction is possible. In contrast, the RBM (MF) and RBM (TAP) approaches show a gradual increase in reconstruction performance as  $\alpha$  increases. Even at  $\alpha = 0.15$ , we see that the characteristic structure of the digit is easily distinguishable. The support is very nearly recovered while the non-zero coefficient values are themselves very inaccurate. At this low measurement rate, we also see that the RBM (TAP) does a much better job at identifying the support of the digit than RBM (MF).

We can also observe the support reconstruction performance independent of the overall NSNR reconstruction performance. This metric is useful for two reasons. In the first, we expect that the RBM model for the support should aide specifically in the support reconstruction performance which then has an effect on the overall NSNR performance, where the on-support coefficients of the signal can be accurately recovered up to  $M = K$ . However, the accuracy of the support recovery itself is not necessarily governed by the same transition, in this case. With the aid of

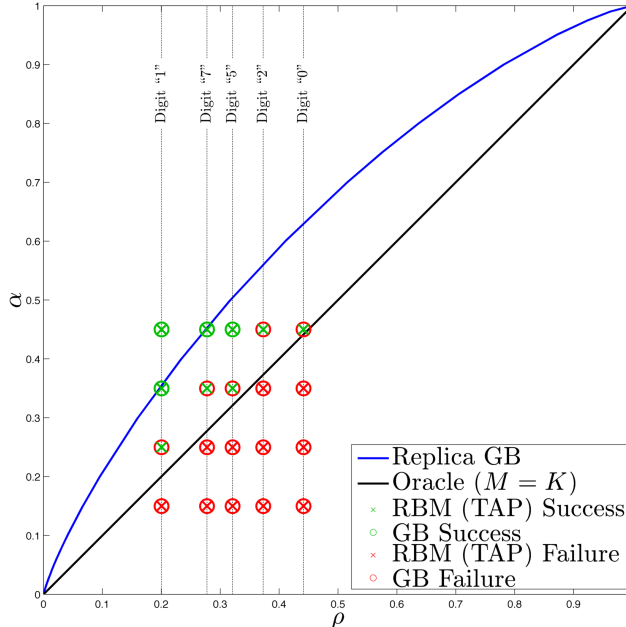


Fig. 2. Comparison between reconstruction success transitions for both AMP-GB and oracle support against the results of Table II. Successful reconstruction of a digit class refers to  $\geq 50\%$  of the tested samples of a class achieving an NSNR  $\leq -15$  dB. Vertical lines represent the average sparsity of a particular digit class.

the RBM support prior, we hope to accurately recover support with arbitrarily good performance constrained only by the power of the RBM to model the support of a given signal. The support recovery performance can be an important aspect of signal reconstruction for recognition tasks which can operate on the signal support independently.

To measure support recovery performance, we compare the true support from the tested handwritten digit samples to the supported estimated when using AMP in conjunction with the GB, RBM (MF), and RBM (TAP) priors. The support recovery for each of these techniques is calculated by comparing the two parts of the partition, the zero and the non-zero part,

$$\frac{\rho_i}{1 - \rho_i} \times \frac{\sum_{x \notin \mathcal{S}} \mathcal{Z}_i^{\text{nz}}}{\sum_{x \in \mathcal{S}} \mathcal{Z}_i^z} \lesssim 1, \quad (33)$$

after the AMP iteration has converged. For the GB prior,  $\rho_i = \rho$ . We choose the Matthews Correlation Coefficient (MCC) [22], which is calculated from the  $2 \times 2$  confusion matrix, to compare the accuracy of this estimated support to the true support. Using the MCC, a value of 1 represents perfect positive correlation,  $-1$  represents perfect negative correlation, and 0 represents a complete lack of correlation. As the MCC can be interpreted as a Pearson correlation coefficient



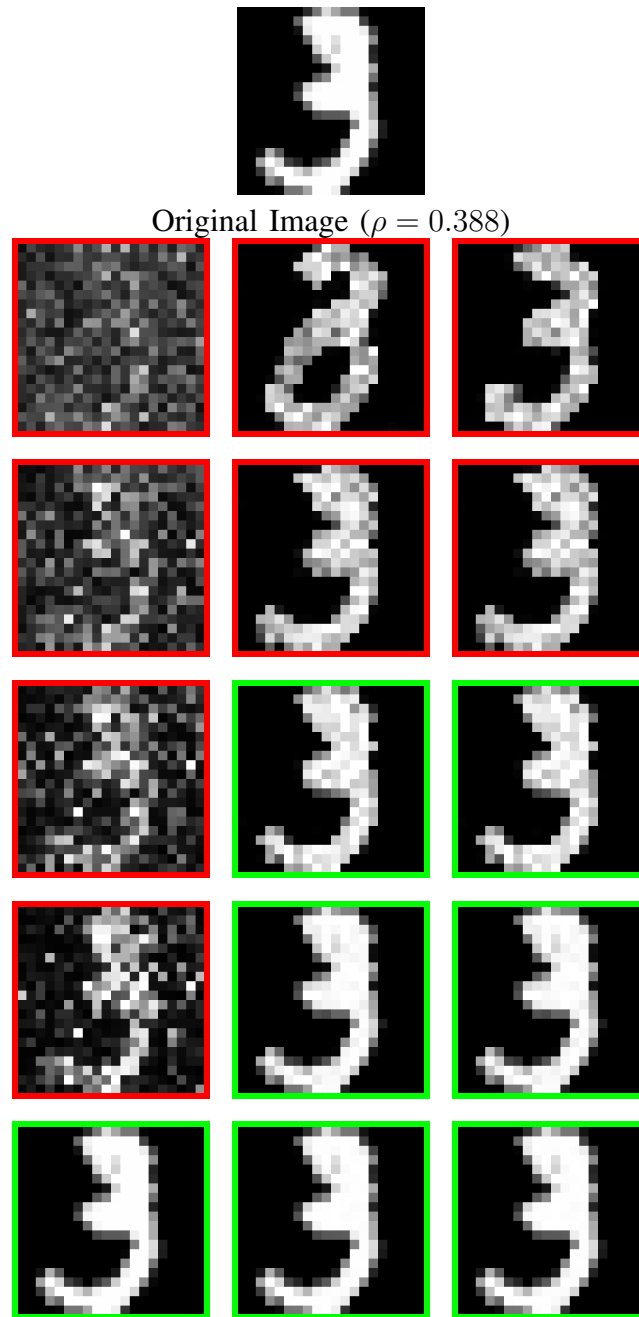


Fig. 3. Reconstruction of a sample image of digit “3” for different subrates (Top to Bottom:  $\alpha = 0.15, 0.25, 0.35, 0.45$ , and  $0.55$ ). Left Column: reconstruction using AMP with GB prior. Middle Column: reconstruction using AMP with RBM (MF). Right Column: reconstruction using AMP with RBM (TAP). Failed reconstructions ( $> -15$  dB NSNR) are indicated with red borders, while successful reconstructions ( $\leq -15$  dB NSNR) are indicated with green borders.

TABLE III

SUPPORT RECOVERY SUCCESS RATES FOR THE HANDWRITTEN DIGIT TEST SET OVER MEASUREMENT RATE FOR DIFFERENT CLASSES OF DIGITS. A SUCCESSFUL SUPPORT RECONSTRUCTION IS DENOTED AS A RECONSTRUCTION WHICH ACHIEVES AN  $MCC \geq 0.70$  WHEN COMPARED TO THE TRUE SUPPORT.

ALL DIGITS	$\alpha$	0.15	0.25	0.35	0.45
GB		0.0%	0.5%	12.1%	52.0%
RBM (MF)		12.4%	60.8%	92.4%	99.9%
RBM (TAP)		24.6%	76.9%	98.1%	100.0%
“1” DIGITS	$\alpha$	0.15	0.25	0.35	0.45
GB		0.0%	3.5%	61.1%	99.1%
RBM (MF)		12.4%	69.0%	92.9%	100.0%
RBM (TAP)		29.2%	86.7%	98.2%	100.0%
“7” DIGITS	$\alpha$	0.15	0.25	0.35	0.45
GB		0.0%	0.0%	18.9%	79.5%
RBM (MF)		13.9%	77.0%	96.7%	100.0%
RBM (TAP)		38.5%	89.3%	100.0%	100.0%
“5” DIGITS	$\alpha$	0.15	0.25	0.35	0.45
GB		0.0%	0.0%	10.3%	63.2%
RBM (MF)		3.4%	29.9%	79.3%	100.0%
RBM (TAP)		3.4%	60.9%	94.3%	100.0%
“2” DIGITS	$\alpha$	0.15	0.25	0.35	0.45
GB		0.0%	0.0%	2.1%	33.0%
RBM (MF)		5.3%	43.6%	83.0%	100.0%
RBM (TAP)		10.6%	63.8%	97.9%	100.0%
“0” DIGITS	$\alpha$	0.15	0.25	0.35	0.45
GB		0.0%	0.0%	0.0%	9.6%
RBM (MF)		22.3%	70.2%	94.7%	100.0%
RBM (TAP)		36.2%	80.9%	97.9%	100.0%

[23], a value of  $MCC \geq 0.7$  represents a strong correlation and we use this value to classify successful support reconstruction.

We can see from Fig. 4 that the RBM (MF) and RBM (TAP) priors provide a very significant enhancement in support recovery performance over the tested handwritten digit samples. We can see that in all cases, the use of the RBM support prior allows for more samples to have their supports reconstructed perfectly ( $MCC = 1$ ). Additionally, a much more significant percentage of the recovered supports exhibit a significant level of correlation. We also observe that the advantage of the RBM (TAP) is clearly present in terms of support recovery performance as compared to the RBM (MF). Finally, we observe the success rates across all tested samples as well as for particular digit classes in Table III.

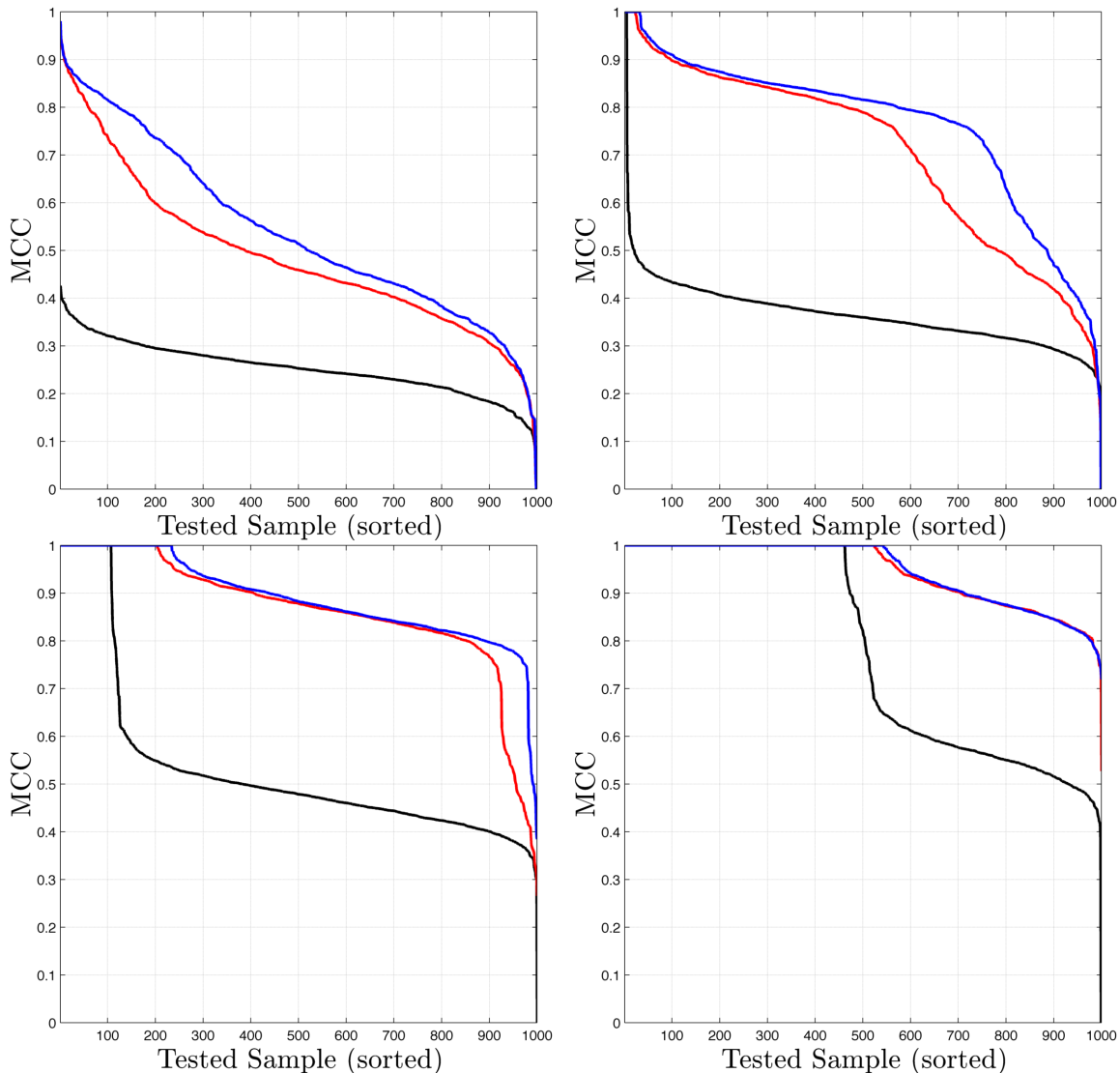


Fig. 4. Comparison over tested MNIST handwritten digits for support detection performance in terms of MCC for  $\alpha = 0.15$  (top left),  $\alpha = 0.25$  (top right),  $\alpha = 0.35$  (bottom left), and  $\alpha = 0.45$  (bottom right). Black curve: AMP using GB prior. Red curve: AMP using RBM (MF) support prior. Blue curve: AMP using RBM (TAP) support prior.

## V. CONCLUSION

In this work we show that using an RBM-based prior on the signal support, when learned properly, can provide CS reconstruction performance superior to that of simple i.i.d. sparsity assumptions for a message passing approach such as AMP. The implications of such an approach are large as these results pave the way for the introduction of much more complex and deep-learned priors. Such priors can be applied to the signal support as we have done here, or further

modifications can be made to adapt the AMP framework to the use of RBMs with real-valued visible layers. Such priors would even aid in moving past the  $M = K$  oracle support transition.

Additionally, the experiments we present here are quite limited, only investigating linear projections observed through an AWGN channel. Much more general, non-linear, observation models can be applied with slight modification to the algorithm, as is done in GAMP. Finally, with the successful application of statistical physics tools to signal reconstruction, as was done in applying TAP to derive AMP, similar approaches could be adapted to produce even better learning algorithms for single and stacked RBMs. Perhaps such future works might allow for the estimation of the RBM model in parallel with signal reconstruction.

#### ACKNOWLEDGMENT

The research leading to these results has received funding from the European Research Council under the European Union's 7<sup>th</sup> Framework Programme (FP/2007-2013/ERC Grant Agreement 307087-SPARCS)

## REFERENCES

- [1] E. Candès and J. Romberg, “Signal recovery from random projections,” in *Computational Imaging III*. San Jose, CA: Proc. SPIE 5674, Mar. 2005, pp. 76–86.
- [2] D. L. Donoho, A. Maleki, and A. Montanari, “Message-passing algorithms for compressed sensing,” *Proc. National Academy of Sciences of the United States of America*, vol. 106, no. 45, p. 18914, 2009.
- [3] M. A. Borgerding and P. Schniter, “Generalized approximate message passing for the cospars analysis model,” *arXiv Preprint*, no. 1312.3968, December 2013.
- [4] S. Rangan, A. K. Fletcher, V. K. Goyal, and P. Schniter, “Hybrid approximate message passing with applications to structured sparsity,” *arXiv preprint arXiv:1111.2581*, 2011.
- [5] G. E. Hinton, “Training products of experts by minimizing contrastive divergence,” *Neural Computation*, vol. 14, no. 8, pp. 1771–1800, August 2002.
- [6] Y. Bengio, “Learning deep architectures for AI,” *Foundations and Trends® in Machine Learning*, vol. 2, no. 1, pp. 1–127, 2009.
- [7] G. Hinton, “A practical guide to training restricted boltzmann machines,” *Momentum*, vol. 9, no. 1, p. 926, 2010.
- [8] J. Pearl, “Reverend Bayes on inference engines: A distributed hierarchical approach,” in *Proceedings American Association of Artificial Intelligence National Conference on AI*, Pittsburgh, PA, USA, 1982, pp. 133–136.
- [9] M. Mézard and A. Montanari, *Information, Physics, and Computation*. OUP, 2009.
- [10] D. L. Donoho, A. Maleki, and A. Montanari, “Message-passing algorithms for compressed sensing: I. motivation and construction,” in *Proceedings of the IEEE Information Theory Workshop*, 2010, p. 1.
- [11] S. Rangan, “Generalized approximate message passing for estimation with random linear mixing,” in *Information Theory Proceedings, IEEE Internaional Symposium on*, 2011, p. 2168.
- [12] J. P. Vila and P. Schniter, “Expectation-maximization gaussian-mixture approximate message passing,” in *Proc. 46th Annual Conference on Information Sciences and Systems*, 2012, p. 1.
- [13] F. Krzakala, M. Mézard, F. Sausset, Y. Sun, and L. Zdeborová, “Statistical physics-based reconstruction in compressed sensing,” *Phys. Rev. X*, vol. 2, p. 021005, 2012.
- [14] ———, “Probabilistic reconstruction in compressed sensing: Algorithms, phase diagrams, and threshold achieving matrices,” *Journal of Statistical Mechanics: Theory and Experiment*, vol. 2012, no. 8, p. P08009, August 2012.
- [15] P. Schniter, “Turbo reconstruction of structured sparse signals,” in *Information Sciences and Systems (CISS), 2010 44th Annual Conference on*. IEEE, 2010, pp. 1–6.
- [16] A. Drémeau, C. Herzet, and L. Daudet, “Boltzmann machine and mean-field approximation for structured sparse decompositions,” *Signal Processing, IEEE Transactions on*, vol. 60, no. 7, pp. 3425–3438, 2012.
- [17] D. J. Thouless, P. W. Anderson, and R. G. Palmer, “Solution of ‘solvable model of a spin-glass’,” *Phil. Mag.*, vol. 35, pp. 593–601, 1977.
- [18] M. Mézard, G. Parisi, and M. A. Virasoro, *Spin Glass Theory and Beyond*. Singapore: World Scientific, 1987.
- [19] J. Yedidia, “An idiosyncratic journey beyond mean field theory,” in *Advanced Mean Field Methods, Theory and Practice*, M. Opper and D. Saad, Eds. The MIT Press, 2001, pp. 21–36. [Online]. Available: <http://www.merl.com/publications/TR2000-027/>
- [20] T. Plefka, “Convergence condition of the TAP equation for the infinite-ranged ising spin glass model,” *Journal of Physics A: Mathematical and General*, vol. 15, no. 6, p. 1971, 1982.

- [21] H. Larochelle and Y. Bengio, "Classification using discriminative restricted boltzmann machines," in *Machine Learning, Proc. Int. Conf. on*, Helsinki, Finland, 2008.
- [22] B. W. Matthews, "Comparison of the predicted and observed secondary structure of T4 phase lysozyme," *Biochimica et Biophysica Acta*, vol. 405, no. 2, pp. 442–451, October 1975.
- [23] D. M. W. Powers, "Evaluation: From precision, recall and F-measure to ROC, informedness, markedness & correlation," *Journal of Machine Learning Technologies*, vol. 2, no. 1, pp. 37–63, 2011.